

# The $\pi$ Donating Ability of Heteroatoms

Fernando Bernardi,\*<sup>1a</sup> Angelo Mangini,\*<sup>1a</sup> Nicolaos D. Epiotis,\*<sup>1b</sup> J. R. Larson,<sup>1b</sup>  
and Sason Shaik<sup>1b</sup>

*Contribution from the Laboratorio C.N.R. dei Composti del Carbonio, Istituto di Chimica Organica, Università di Bologna, Bologna, Italy, and the Department of Chemistry, University of Washington, Seattle, Washington 98195. Received December 9, 1976*

**Abstract:** The  $\pi$  donating ability of heteroatoms in diverse systems such as  $^+\text{CH}_2\text{X}$ ,  $\text{C}_6\text{H}_5\text{X}$ ,  $\text{CH}_2=\text{CHX}$ , and  $\text{CH}\equiv\text{CX}$  has been studied by means of SCFMO ab initio computations at the STO-3G and 4-31G levels. The results indicate that the  $\pi$  donating ability of first-row heteroatoms is larger than that of the second-row heteroatoms in systems where the adjacent fragment has a high-lying LUMO. On the other hand, the trend reverses when the adjacent fragment has a low-lying LUMO. A qualitative MO rationalization of these trends is offered and experimental evidence in support of the qualitative arguments is discussed.

## I. Introduction

The manner in which substituents affect the electronic properties of the parent substrate is an important problem of organic chemistry. While a great deal has been learned by means of experimental studies, recent theoretical investigations suggest that the problem may be more complex than it appears. For example, we recently reported that the  $\pi$  donating ability of S is greater than that of O with respect to an adjacent carbocationic fragment, a result which is in opposition to the "accepted" viewpoint.<sup>2a</sup> Consequently, we decided to investigate the problem in a systematic manner and attempt to answer the question of whether substituent effects are dependent on the electronic nature of the parent substrate. The results are presented below along with a discussion of their implications for organic chemistry.

## II. Ab Initio Computations

The method employed has been a single determinant LCAO-MO-SCF procedure in which each MO is expressed as a linear combination of a set of contracted Gaussian type functions. All computations have been carried out with the Gaussian 70 series of programs.<sup>3</sup> In discussing the  $\pi$ -donating ability of heteroatoms, we shall make use of quantities like gross atomic charges and gross AO populations that are obtained according to Mulliken population analysis. Because of the limitations of such procedure, the related quantities can provide meaningful trends only if they are obtained at the same computational level. Since we have included in the investigation molecular species of the size of substituted benzenes, which are too large to be studied ab initio with an extended basis set, we have carried out the computations using a minimal basis set (STO-3G).<sup>4a</sup> However, in the case of the simplest molecules investigated here, we have also obtained data at the extended level for testing the reliability of the results obtained at the minimal level.

**Substituted Methyl Cations.** In a previous paper,<sup>2a</sup> we have reported the geometries of  $^+\text{CH}_2\text{XH}$  ( $\text{X} = \text{O}, \text{S}$ ) and  $^+\text{CH}_2\text{X}$  ( $\text{X} = \text{F}, \text{Cl}$ ) species computed at the 4-31G<sup>4b</sup> level. Here, the geometries of these cations have been recomputed at the STO-3G level and the corresponding results are listed in Table I. It is noteworthy that the geometric parameters obtained at two different levels of computation are in agreement.

**Ethylene Derivatives.** The molecular species  $\text{CH}_2=\text{CHXH}$  ( $\text{X} = \text{O}, \text{S}$ ) and  $\text{CH}_2=\text{CHX}$  ( $\text{X} = \text{F}, \text{Cl}$ ) were computed and the results are listed in Table II. In the case of  $\text{CH}_2=\text{CHOH}$  and  $\text{CH}_2=\text{CH}_2\text{SH}$ , the cis conformation is found to be more stable (ca. 2 and 1 kcal/mol, respectively). These two molecules have also been the object of a recent ab initio investigation

at an extended level<sup>5</sup> and the obtained results compare very favorably with those of the present work.

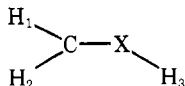
**Benzene Derivatives.** The monosubstituted benzenes  $\text{C}_6\text{H}_5\text{XH}$  ( $\text{X} = \text{O}, \text{S}$ ) and  $\text{C}_6\text{H}_5\text{X}$  ( $\text{X} = \text{F}, \text{Cl}$ ) were computed. In these molecules we have optimized the distance of the bond connecting the substituent to the benzene ring. The computed values are listed in Table III. It is interesting to point out that these bond lengths are similar to those obtained in the ethylene derivatives.

**Acetylene Derivatives.** The molecular species  $\text{HC}\equiv\text{CXH}$  ( $\text{X} = \text{O}, \text{S}$ ) and  $\text{HC}\equiv\text{CX}$  ( $\text{X} = \text{F}, \text{Cl}$ ) were computed. The C-C and C-X bond lengths were optimized while the remaining parameters were kept fixed at standard values. The computed geometric parameters are listed in Table IV. It is interesting to point out that the C-X bond lengths are shorter than those in ethylene or benzene derivatives.

**The  $\pi$ -Donating Ability of Oxygen and Sulfur.** We first focus our attention on the charge transfer occurring between the two moieties R and XH in the oxygen and sulfur molecular species under investigation. The relevant data are shown in Figure 1. In all cases, the gross charge of the XH moiety represents the amount of electronic charge transferred to (+) or from (-) the R fragment as the result of the interaction between the two fragments. The values for the  $\pi$  electron transfers have been computed from the gross orbital populations of the carbon  $2p_\pi$  orbitals. The values quoted in Figure 1 are merely the differences  $q_1^\pi - q_0^\pi$ , where  $q_1^\pi$  and  $q_0^\pi$  are the gross orbital populations of the carbon  $2p_\pi$  orbitals in R after and prior to interaction, respectively. These values measure the amount of electronic charge transferred to the  $\pi$  system and they constitute a measure of the  $\pi$ -donating ability of the various groups. The values for the  $\sigma$  components are obtained from the values of the total and  $\pi$  electron populations.

The following observations can be made: (a) When  $\text{X} = \text{S}$  both the  $\sigma$  and  $\pi$  electron transfer occur in the same direction, i.e., from the heteroatom to the adjacent system. (b) When  $\text{X} = \text{O}$  the  $\pi$  donation occurs always from the heteroatom to the adjacent system while  $\sigma$  electron transfer occurs always in the opposite direction. (c) The extent of  $\pi$  electron transfer is much more sensitive to the adjacent system than that of the  $\sigma$  electron transfer. (d) The values of Figure 1, when R is  $\text{CH}_2=\text{CH}$  and  $\text{C}_6\text{H}_5$ , are almost identical. This suggests that, for this kind of problem, a phenyl fragment can be replaced by an ethylene fragment.

We have also carried out computations of  $^+\text{CH}_2\text{XH}$  and  $\text{CH}_2=\text{CHX}$  at the 4-31G level in order to see if the previous trends hold. The results are shown in Figure 2. It can be seen that there is qualitative agreement with the previous findings

**Table I.** STO-3G Geometric Parameters<sup>a</sup> for <sup>+</sup>CH<sub>2</sub>XH and <sup>+</sup>CH<sub>2</sub>X Carbocations


Parameters in <sup>+</sup> CH <sub>2</sub> XH and <sup>+</sup> CH <sub>2</sub> X	X			
	O <sup>b</sup>	S	F <sup>b</sup>	Cl
<i>r</i> (C-X)	1.271	1.630	1.265	1.677
<i>r</i> (C-H <sub>1,2</sub> )	1.114	1.101	1.127	1.119
<i>r</i> (X-H <sub>3</sub> )	1.003	1.353		
∠H <sub>1</sub> CH <sub>2</sub>	120.6	116.4	122.7	121.1
∠CXH <sub>3</sub>	114.7	97.8		

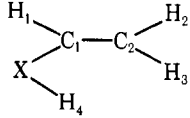
<sup>a</sup> Bond lengths in Å and angles in degrees. <sup>b</sup> Reference 5.

although the absolute quantities can differ significantly (e.g., the  $\sigma$  charge transfers).

**The  $\pi$ -Donating Ability of Fluorine and Chlorine.** The gross charges of the two interacting fragments and the corresponding  $\pi$  and  $\sigma$  charge transfers computed at the STO-3G level for the various fluoro and chloro derivatives investigated here are presented in Figure 3. According to these results both heteroatoms act as  $\pi$  donors and  $\sigma$  acceptors, with fluorine being the best  $\pi$  donor in all cases. However, the comparison with the 4-31G results (see Figure 4) shows that, in the substituted methyl cations, chlorine is a better  $\pi$  donor than fluorine, in contrast with the previous STO-3G results. In the ethylene derivatives, fluorine is a better  $\pi$  donor than chlorine, in agreement with the previous STO-3G results. These results, obtained with a more rigid basis set optimized for the neutral atoms, seem less reliable for the cations than the 4-31G results obtained with a more flexible basis set. Therefore, we can conclude that in <sup>+</sup>CH<sub>2</sub>X systems (X = F, Cl), the second-row heteroatom is a better donor while the trend reverses in CH<sub>2</sub>=CHX, CH≡CX, and C<sub>6</sub>H<sub>5</sub>X.

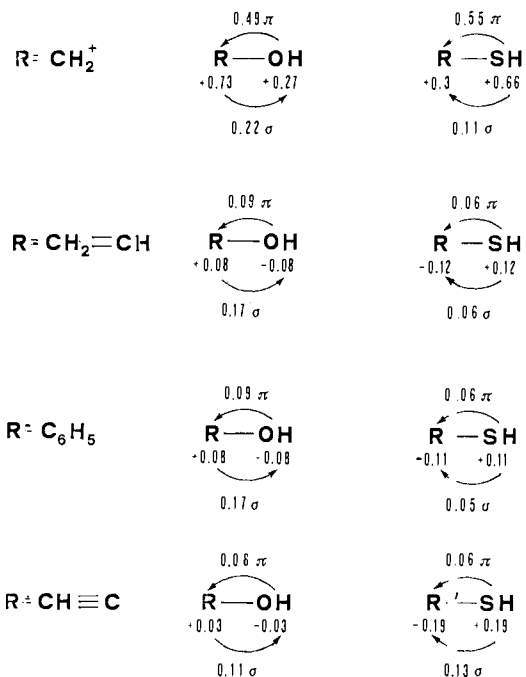
**A Qualitative MO Model for Substituent Effects.** The most important result of the ab initio calculations is the demonstration that, in <sup>+</sup>CH<sub>2</sub>XH (X = O, S), the second-row heteroatom is a better donor. By contrast, the trend reverses in CH<sub>2</sub>=CHXH, CH≡CXH, and C<sub>6</sub>H<sub>5</sub>XH systems. A similar trend can be discussed in the comparison of F and Cl. Is there any simple way to interpret these interesting trends?

In recent years, there has been a burst of activity in the field of chemistry which can now be labeled theoretical organic chemistry.<sup>7</sup> In particular, a successful rationalization of various structural and reactivity trends has been shown to be possible by focusing on the stabilizing MO interactions which obtain in the two systems under comparison. These are evaluated on the basis of eq 1.

**Table II.** STO-3G Total Energies and Geometric Parameters of CH<sub>2</sub>=CHX (X = F, Cl) and CH<sub>2</sub>=CHXH (X = O, S)<sup>a</sup>


Parameters	X = O		X = S		X = F	X = Cl
	Cis <sup>b</sup>	Trans <sup>b</sup>	Cis <sup>b</sup>	Trans <sup>b</sup>		
<i>r</i> (C <sub>1</sub> -C <sub>2</sub> )	1.316	1.311	1.313	1.311	1.316	1.312
<i>r</i> (C <sub>1</sub> -X)	1.392	1.395	1.758	1.764	1.356	1.774
<i>r</i> (X-H)	0.989	0.989	1.332	1.332		
∠H <sub>1</sub> C <sub>1</sub> C <sub>2</sub>	124.7	121.5	120.1	118.6	122.2	123.7
∠XC <sub>1</sub> C <sub>2</sub>	125.5	122.4	126.9	124.7	124.4	124.5
∠H <sub>4</sub> XC <sub>1</sub>	105.4	105.6	95.9	95.6		
Total energy	-150.91567	-150.91239	-470.25617	-470.25459	-174.53246	-531.07785

<sup>a</sup> Bond lengths in Å and angles in degrees. <sup>b</sup> Cis and trans with respect to the C-C bond.

**Figure 1.** Gross charges of the R and XH moieties computed at the STO-3G level, together with the  $\sigma$  and  $\pi$  electron transfers.

$$SE = 2 \frac{H_{ij}^2}{\delta\epsilon_{ij}} \quad (1)$$

Here, the stabilization energy (SE) refers to the interaction of a doubly occupied orbital  $\phi_i$  and an unoccupied orbital  $\phi_j$ .  $H_{ij}$  is the corresponding interaction matrix element with respect to an effective one-electron Hamiltonian and  $\delta\epsilon_{ij}$  the corresponding energy gap between the two orbitals ( $\epsilon_i - \epsilon_j$ ). Destabilizing MO interactions should also be considered, but, in most cases, their neglect does not alter the qualitative conclusion.

For the problem at hand, the relevant orbital interaction is that between the  $\pi$  lone pair of the heteroatom and the lowest unoccupied MO (LUMO) of the adjacent substrate. The corresponding interaction matrix element,  $H_{ij}$ , can be expanded in terms of interaction matrix elements between AO's,  $h_{mn}$ , which are approximated by the Wolfsberg-Helmholz expression:<sup>8</sup>

$$h_{mn} = 1/2K(\beta_A^m + \beta_B^n)S_{mn} \quad (2)$$

Here  $K$  is a constant,  $\beta_A^m$  and  $\beta_B^n$  are equated to the negative values of the valence orbital ionization energies of the AO's

**Table III.** STO-3G Geometric Parameters of  $C_6H_5X$  ( $X = F, Cl$ ) and  $C_6H_5XH$  ( $X = O, S$ )

X	$r(C-X)$ , Å
O	1.395
S	1.770
F	1.357
Cl	1.775

**Table IV.** STO-3G Geometric Parameters of  $HC\equiv CX$  ( $X = F, Cl$ ) and  $HC\equiv CXH$  ( $X = O, S$ )

	X = O	X = S	X = F	X = Cl
$r(C_1-X)$ , Å	1.350	1.704	1.319	1.708
$r(C_1-C_2)$ , Å	1.168	1.171	1.167	1.169

**Table V.** Overlap Integrals ( $S_{ij}$ ) and Interaction Matrix Elements ( $H_{ij}$ ) of the Heteroatom Lone Pair and the LUMO of the Adjacent  $\pi$  Systems

System	CNDO/2		STO-3G	
	$S_{ij}$	$H_{ij}$	$S_{ij}$	$H_{ij}$
$^+CH_2OH$	0.2031	-5.4451	0.1864	-4.9982
$^+CH_2SH$	0.2017	-4.9049	0.1636	-3.9782
$CH_2=CHOH$	0.0969	-1.7475	0.1082	-1.9520
$CH_2=CHSH$	0.1022	-1.5886	0.0935	-1.4532
$C_6H_5OH$	0.0788	-1.4208	0.0866	-1.5629
$C_6H_5SH$	0.0808	-1.2567	0.0729	-1.1334
$CH\equiv COH$	0.1091	-1.9682	0.1278	-2.3052
$CH\equiv CSH$	0.1175	-1.8260	0.1131	-1.7579

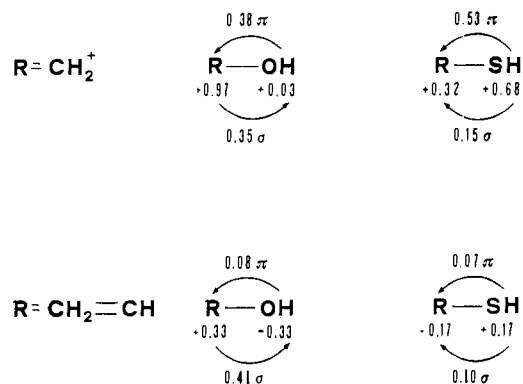
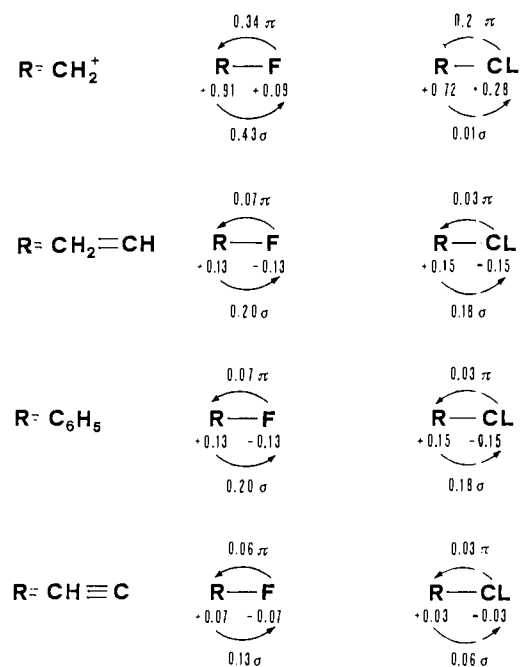
**Table VI.** Lone Pair Ionization Potentials (IP) and Estimated  $\delta\epsilon_{ij}$  Values<sup>a</sup>

Model ( $H_2X, HX$ )	IP, <sup>b</sup> eV	$\delta\epsilon_{ij}$	$\delta\epsilon_{ij}$
		( $^+CH_2XH,$ $^+CH_2X$ )	( $CH_2=CHXH,$ $CH_2=CHX$ )
HF	16.4	8.11	20.84
HCl	12.80	5.14	17.87
H <sub>2</sub> O	12.61	4.95	17.68
H <sub>2</sub> S	10.48	2.82	15.55

<sup>a</sup> The  $\delta\epsilon_{ij}$  values have been computed from the IP values and from LUMO energies computed at the 4-31G level. <sup>b</sup> Taken from ref 10.

$m$  and  $n$  of A and B, and  $S_{mn}$  is the overlap integral between the same AO's. The corresponding energy gap,  $\delta\epsilon_{ij}$ , can be estimated by reference to the lone pair ionization potential of the heteroatoms and the electron affinity of the adjacent substrates or by explicit calculation of the energies of the appropriate MO's

We can now consider the relative  $\pi$ -donating ability of OH and SH with respect to  $CH_2=CH-$  and  $^+CH_2-$  as a specific example. In this case, the  $H_{ij}$  term will favor greater  $\pi$  donation by O (see Table V), not necessarily because the  $S_{CO}$  overlap is greater than  $S_{CS}$  overlap, as is generally believed, but because the  $(\beta_A + \beta_B)$  term in eq 2 favors OH to a greater extent than the overlap integral may favor SH. On the other hand, the  $\delta\epsilon_{ij}$  term favors SH over OH owing to the lower ionization potential of the S3p lone pair as compared with the O2p lone pair (see Tables VI and VII). Equation 1 suggests that one may encounter two extreme situations: (a) When the LUMO of the central fragment lies high in energy, the variation of  $H_{ij}$  will dominate that of  $\delta\epsilon_{ij}$  and OH will be a better donor. A system where this order is found is  $CH_2=CHX$ , where  $X = OH, SH$ . (b) When the LUMO of the central fragment lies low in energy, the variation in the energy gap will dominate, and, thus,

**Figure 2.** Gross charges of the R and XH moieties computed at the 4-31G level, together with the  $\sigma$  and  $\pi$  electron transfers.**Figure 3.** Gross charges of the R and X moieties computed at the STO-3G level, together with the  $\sigma$  and  $\pi$  electron transfers.

SH will be the better donor. This order is found in  $^+CH_2X$  ( $X = OH, SH$ ).

An inspection of the lone pair ionization potentials and  $H_{ij}$ <sup>9</sup> data shown in Tables V–VII will convince the reader that, in general, any comparison of a first-row element and a second-row element belonging to the same column of the periodic table is subject to matrix element or energy gap control because in all such problems, the numerator and denominator of eq 1 work in opposite directions. Our results indicate that in molecules like  $CH_2=CHX$ ,  $CH\equiv CX$ , and  $C_6H_5X$ , where  $\delta\epsilon_{ij}$  is very large, the relative extent of  $\pi$  charge transfer is controlled by the  $H_{ij}$  term and, e.g., oxygen is a better  $\pi$  donor than sulfur. By contrast, in species such as  $^+CH_2X$ , where  $\delta\epsilon_{ij}$  is very small, the relative extent of  $\pi$  charge transfer is controlled by the  $\delta\epsilon_{ij}$  term and sulfur becomes now a better  $\pi$  donor than oxygen.

We are now prepared to compare these theoretical results with actual experimental data. Specifically, the degree of  $\pi$  interaction between R and X is reflected in three theoretical quantities: (a)  $\pi$  charge transfer from X to R, which is related to the quantity  $(H_{ij}/\delta\epsilon_{ij})^2$ . (b)  $\pi$  LUMO energy of RX, which is related to the quantity  $(H_{ij}^2/\delta\epsilon_{ij})$ . (c) The  $\pi$  R–X bond order (or overlap population), which is related to the quantity  $H_{ij}/\delta\epsilon_{ij}$  (or  $H_{ij}S_{ij}/\delta\epsilon_{ij}$ ). Each theoretical quantity is connected to experimental observables in the following manner:

Table VII. STO-3G and 4-31G (in Parentheses) LUMO Energies of Various  $\pi$  Systems and Estimated  $\delta\epsilon_{ij}$  Values

R	LUMO <sup>a</sup>	$\delta\epsilon_{ij}$ <sup>a</sup>			
		X = O	X = S	X = F	X = Cl
+CH <sub>2</sub> -	-6.36 (-7.66)	4.31 (5.91)	1.20 (2.75)	6.24 (9.42)	5.07 (5.11)
C <sub>6</sub> H <sub>5</sub> -	+7.27	17.93	14.83	19.87	18.70
CH <sub>2</sub> =CH-	+8.93 (5.06)	19.60 (18.65)	16.49 (15.48)	21.53 (22.14)	20.36 (17.83)
CH≡C-	+11.18	21.85	18.74	23.78	22.61

<sup>a</sup> All values are expressed in eV.

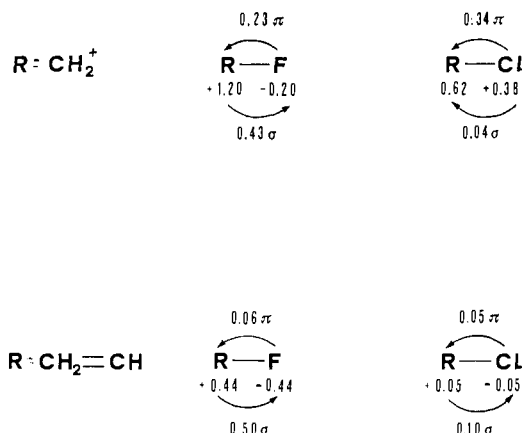


Figure 4. Gross charges of the R and X moieties computed at the 4-31G level, together with the  $\sigma$  and  $\pi$  electron transfers.

(a)  $\pi$  charge transfer from X to R is related to the  $\pi$  electron densities of the atoms which constitute R. In general, experimental techniques are available which provide measures of the total i.e.,  $\pi$  and  $\sigma$  atomic electron densities. A commonly used method of this type is <sup>13</sup>C NMR spectroscopy. Clearly, one should be able to assess independently  $\sigma$  atomic electron densities if such a method is to be used in studying  $\pi$  electron densities. This can be accomplished only by reference to a model and the latter differs in various investigations. As a result, these experimental methods are not ideal for studying the R-X  $\pi$  interaction.

(b) The  $\pi$  R-X bond order is an index of the R-X  $\pi$  bond strength. Assuming that relative R-X  $\pi$  bonding determines the relative stability of a series of RX molecules, where X is the variable group, the relative  $\pi$  R-X bond order constitutes a measure of the relative stabilization of R by X. This can be probed by studying the thermodynamics of reactions producing RX. Experimental bond lengths can be obtained from spectroscopic measurements. These methods are satisfactory for studying the  $\pi$  R-X interaction under the stated assumption.

(c) The  $\pi$  LUMO energy of RX, which is nothing else but the perturbed  $\pi$  LUMO of R, is related to the electron affinity and reduction potential of RX, both of which can be measured experimentally. In addition, the  $\pi$  LUMO energy of RX is related indirectly to the following two properties:

(1) The Lewis acidity of RX in its reaction to form a weak molecular complex. The stability of such a complex, e.g., a charge-transfer complex, a hydrogen-bonded complex, etc., is related to the stabilization resulting from the interaction of the HOMO of the donor partner and the LUMO of the acceptor partner, which, in turn, is related to the corresponding HOMO-LUMO energy gap in R and X. Accordingly, as RX becomes a better  $\pi$  acceptor, stronger  $\pi$  complexes are expected to be formed with  $\pi$  donors. As a result, the heat of formation of a weak complex provides information about the LUMO energy of RX.

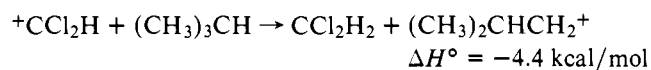
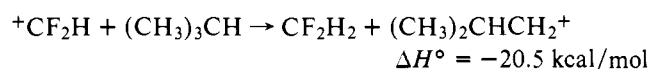
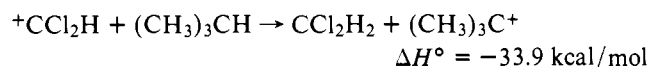
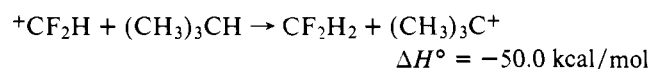
(2) The intermolecular reactivity of RX, where RX acts as

the acceptor. Specifically, it is well known that this can be correlated with the energy gap between the HOMO of the donor reactant and the LUMO of the acceptor reactant.<sup>11</sup> Under this assumption, the corresponding rate constant is a measure of the LUMO energy of RX.

In short, electron affinity and reduction potential are roughly one-orbital properties. Weak complex stability as well as intermolecular reactivity may also be so. Hence, experimental techniques geared to measure these properties are very well suited for studying the  $\pi$  R-X interaction because they can provide information about the  $\pi$  LUMO of RX which is connected with the R-X  $\pi$  interaction.

Recalling that, as the R-X interaction increases,  $\pi$  charge transfer from X to R, the  $\pi$  LUMO energy of RX, and the  $\pi$  R-X bond order all increase,<sup>12</sup> we can now survey typical experimental data. Although <sup>13</sup>C NMR data relating to atomic electron density cannot be utilized to discern the relative magnitude of  $\pi$  effects, owing to the superposition of  $\sigma$  effects, they can be useful insofar as they can be correlated with the results of the ab initio computations. Typical <sup>13</sup>C NMR results are displayed in Table VIII. Here, when the parent substrate R has a high-lying  $\pi$  LUMO, as is the case for benzene, ethylene, and acetylene, the expected order of  $\pi$  donation is F > Cl > ... RO > RS > ... , etc. The experimental results show that this order does materialize in the positions which are mostly affected by  $\pi$  donation, i.e., position 2 in substituted ethylene and acetylene, and positions 2 and 4 in substituted benzene. On the other hand, the positions which are affected more by the inductive effect, namely, position 1 in substituted ethylene and acetylene and positions 1 and 3 in substituted benzene, show the reverse order. <sup>13</sup>C NMR studies of cations in solution have been reported<sup>13</sup> but they cannot be unambiguously interpreted because consideration of inductive effects would predict a similar trend.

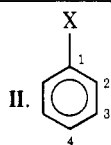
Thermodynamic data of the type displayed below<sup>14a</sup> are more informative insofar as  $\pi$  interactions are concerned. Specifically, we expect that when the parent substrate has a low-lying AO, as is the case for <sup>+</sup>CH<sub>3</sub>, the expected order of  $\pi$  interaction is Br > Cl > F ... , etc., and the attendant stabilization of <sup>+</sup>CH<sub>2</sub>- by the heteroatom should vary in the same direction. The gas-phase enthalpies of the reactions shown below are in accord with our predictions, if it is assumed that enthalpic trends are primarily determined by the relative stability of the carbocations (e.g., <sup>+</sup>CF<sub>2</sub>H) rather than the corresponding halohydrocarbons (e.g., CH<sub>2</sub>F<sub>2</sub>).



The observation that  $\Delta H^\circ$  is  $\sim 1.1$  eV more negative for X =

**Table VIII.**  $^{13}\text{C}$  Chemical Shift ( $\delta_{\text{Me}_4\text{Si}}$ ) Values<sup>a</sup> for Substituted Ethylene, Benzene, and Acetylene

X	1. $\text{H}_2\text{C}=\text{CHX}$ $\delta$ ppm		Ref
	1	2	
Cl	126.1	117.4	<i>b</i>
Br	115.6	122.1	<i>b</i>
I	85.4	130.5	<i>b</i>

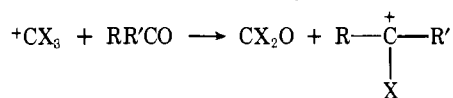


X	II. $\delta$ ppm				Ref
	1	2	3	4	
OH	154.9	115.4	129.7	121.0	<i>c</i>
SH	130.7	129.2	128.9	125.4	<i>c</i>
F	163.8	114.4	129.6	124.3	<i>d</i>
Cl	134.3	128.6	129.8	126.5	<i>c</i>
OCH <sub>3</sub>	160.2	114.1	129.5	120.7	<i>c</i>
SCH <sub>3</sub>	138.4	126.5	128.6	124.8	<i>c</i>

X	III. $\text{H}-\text{C}\equiv\text{CX}$ $\delta$ ppm		Ref
	1	2	
OC <sub>2</sub> H <sub>5</sub>	88.2	22.0	<i>e</i>
SC <sub>2</sub> H <sub>5</sub>	71.4	80.2	<i>e</i>

<sup>a</sup> Larger value indicates a more positively charged carbon. <sup>b</sup> G. E. Maciel, *J. Phys. Chem.*, **69**, 1947 (1965). <sup>c</sup> L. F. Johnson and W. C. Jankowski, "Carbon-13 NMR Spectra", Wiley-Interscience, New York, N.Y., 1972. <sup>d</sup> A. J. Gordon and R. A. Ford, "The Chemist's Companion", Wiley-Interscience, New York, N.Y., 1972. <sup>e</sup> D. Rosenberg, J. W. De Haan, and W. Drenth, *Recl. Trav. Chim. Pays-Bas*, **87**, 1387 (1968).

F than for X = Cl, in the reaction shown below,<sup>14b</sup> is also in accord with our predictions, assuming that enthalpic trends reflect primarily the relative stability of  $^+\text{CX}_3$ .



Turning our attention to data connected with  $\pi$  LUMO energies, we note that the rate data shown in Table IX are consistent with the order Cl > F with respect to  $\pi$  interaction with the carbocationic center. In addition, the greater selectivity of hydride abstraction by  $^+\text{CCl}_2\text{H}$  than for  $^+\text{CF}_2\text{H}$ <sup>14a</sup> is understandable if it is assumed that higher reactivity, signaled by a lower LUMO energy, implies lower selectivity (Hammond's postulate).<sup>15</sup> Here, a greater  $^+\text{C}-\text{Cl}$  interaction produces a higher energy  $^+\text{CCl}_2\text{H}$  LUMO and a less reactive  $^+\text{CCl}_2\text{H}$  carbocation. Finally, it should also be noted that the  $\pi$  bonding ability of a heteroatomic atom adjacent to an excited substrate, which features low-lying singly occupied bonding MO, has been determined to be S > O on the basis of experiments.<sup>16</sup>

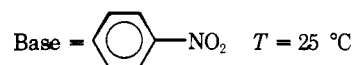
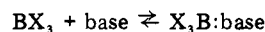
Boron has a high lying vacant 2p AO and, hence, the  $\pi$  interaction between B and a heteroatom X is predicted to vary in the order B-F > B-Cl > B-Br > B-I. Accordingly, the Lewis acidity of  $\text{BX}_3$  molecules is expected to vary in the order  $\text{BI}_3 > \text{BBr}_3 > \text{BCl}_3 > \text{BF}_3$ . Experimental results are in agreement with this prediction. Typical data<sup>17</sup> are shown below

**Table IX.** Gas-Phase Rate Coefficient of Hydride Abstraction from Linear Hydrocarbons by Halo Carbocations ( $k \times 10^{10}$ ,  $\text{cm}^3 \text{mol}^{-1} \text{s}^{-1}$ )<sup>a</sup>

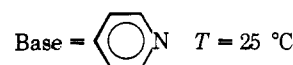
Hydro-carbon	Carbocations			
	$^+\text{CF}_2\text{H}$	$^+\text{CCl}_2\text{H}$	$^+\text{CF}_3$	$^+\text{CCl}_3$
<i>n</i> -C <sub>4</sub> H <sub>10</sub>	11.8 ± 0.4	4.6 ± 0.3	7.5 ± 0.7	
<i>n</i> -C <sub>5</sub> H <sub>12</sub>	13.1 ± 0.3	6.1 ± 0.2	8.9 ± 0.4	
<i>n</i> -C <sub>7</sub> H <sub>16</sub>	15.0 ± 0.4	10.0 ± 0.6		
<i>n</i> -C <sub>8</sub> H <sub>18</sub>			13.7 ± 0.5	0.76 ± 0.1

<sup>a</sup> S. G. Lias, J. R. Eyler, and P. Ausloos, *Int. J. Mass Spectrom. Ion Phys.*, **19**, 219 (1976).

and more supporting evidence can be found in the literature.<sup>18</sup>



X	$-\Delta H^\circ$
F	6.7 ± 0.5
Cl	9.7 ± 0.2
Br	12.5 ± 0.2



X	$-\Delta H^\circ$
F	25.0 ± 1.0
Cl	30.8 ± 0.2
Br	32.0 ± 0.2

At this point, it should be mentioned that any data related to carbocations in solution, unlike the gas phase data discussed above, cannot be interpreted in an unambiguous manner unless the coordination properties of the carbocations are known.

### III. Conclusions

The ideas described in this work may have wide applicability to chemical problems and they seem to be related to the hard-soft acid-base correlation.<sup>19</sup> In particular, the unsaturated moiety, i.e.,  $^+\text{CH}_2^-$ ,  $\text{CH}_2=\text{CH}^-$ ,  $\text{CH}\equiv\text{C}^-$ , and  $\text{C}_6\text{H}_5^-$ , is the  $\pi$  Lewis acid and the heteroatom is the  $\pi$  Lewis base. A hard-hard interaction obtains when the HOMO-LUMO energy gap is large and the variation of the stabilization energy is dominated by the interaction matrix element. On the other hand, a soft-soft interaction obtains when the HOMO-LUMO energy gap is small and controls the variation of the stabilization energy.

In connection with the above discussion, it should be noted that attempts to provide a theoretical basis for this correlation have been made and a distinction between frontier controlled and charge controlled interactions has been proposed by Klopman.<sup>20</sup> Our conclusions are different insofar as we distinguish energy gap vs. matrix element frontier control of interaction. This difference is conveyed by means of the ideogram shown below.

Size of HOMO-LUMO energy gap ( $\delta\epsilon$ )	Dominant effect	
	Klopman	This work
Large	Charge interaction	$H^2/\delta\epsilon$ Variation dominated by $H$
Small	$H^2/\delta\epsilon$	$H^2/\delta\epsilon$ Variation dominated by $\delta\epsilon$

Of course, coulombic effects may become important irrespective of the size of  $\delta\epsilon$ . Clearly, more experimental and

theoretical work designed to test directly these ideas is needed before a final picture emerges.

**Acknowledgment.** This work was supported by the Graduate School Research Fund of the University of Washington and NATO Fellowships to N.D.E. and F.B. N.D.E. is an A. P. Sloan Fellow (1976–1978).

## References and Notes

- (1) (a) Università di Bologna; (b) University of Washington.
- (2) (a) F. Bernardi, I. G. Csizmadia, and N. D. Epiotis, *Tetrahedron*, **31**, 3085 (1975); (b) F. Bernardi, N. D. Epiotis, and R. Yates, *J. Am. Chem. Soc.*, **97**, 1334 (1975); (c) R. Yates, N. D. Epiotis, and F. Bernardi, *ibid.*, **97**, 4198 (1975); (d) N. D. Epiotis, R. Yates, and F. Bernardi, *ibid.*, **97**, 4198 (1975); (e) F. Bernardi, N. D. Epiotis, and R. Yates, *ibid.*, **97**, 6615 (1975).
- (3) W. J. Hehre, W. A. Lathan, R. Ditchfield, M. D. Newton, and J. A. Pople, Program No. 236, Quantum Chemistry Program Exchange, Indiana University, Bloomington, Ind.
- (4) (a) W. J. Hehre, R. F. Stewart, and J. A. Pople, *J. Chem. Phys.*, **51**, 2657 (1969); (b) R. Ditchfield, W. J. Hehre, and J. A. Pople, *ibid.*, **54**, 725 (1971).
- (5) W. A. Lathan, L. A. Curtiss, W. J. Hehre, J. B. Lisle, and J. A. Pople, *Prog. Phys. Org. Chem.*, **11**, 175 (1974).
- (6) S. Samdal and H. M. Seip, *J. Mol. Struct.*, **28**, 193 (1975).
- (7) N. D. Epiotis, W. R. Cherry, S. Shaik, R. L. Yates, and F. Bernardi, *Top. Curr. Chem.*, **70** (1977).
- (8) M. Wolfsberg and L. Helmholz, *J. Chem. Phys.*, **20**, 837 (1952).
- (9) As is shown in Table V, the trend of the overlap integrals depends on the basis set, while the trend in the  $H_{ij}$ 's is not basis set dependent.
- (10) (a) "Ionization Potentials, Appearance Potentials, and Heats of Formation of Gaseous Positive Ions", National Bureau of Standards, NBS 26, 1969; (b) A. D. Baker and D. Betteridge, "Photoelectron Spectroscopy", Pergamon Press, Elmsford, N.Y., 1972.
- (11) See K. Fukui, *Acc. Chem. Res.*, **4**, 57 (1971); G. Klopman, Ed., "Chemical Reactivity and Reaction Paths", Wiley-Interscience, New York, N.Y., 1974; R. F. Hudson, *Angew. Chem., Int. Ed. Engl.*, **12**, 36 (1973).
- (12) The quantities  $(H_{ij}/\delta\epsilon)^2$  or  $(H_{ij}/\delta\epsilon^2)$  and  $H_{ij}^2/\delta\epsilon$  involve the interaction matrix element and the energy gap factors acting in competition. However, the balance in this competition is different in the two quantities. Accordingly, solutions may exist where indices related to  $(H_{ij}/\delta\epsilon)^2$  or  $(H_{ij}/\delta\epsilon)$  vary in one manner, while the indices related to  $(H_{ij}^2/\delta\epsilon)$  vary by exactly the opposite manner. Our computations show that the relative ordering of F and Cl and well as OH and SH remains unaltered in all indices in all systems examined.
- (13) H. Volz and W. D. Mayer, *Justus Liebig's Ann. Chem.*, 835 (1975); G. A. Olah, Y. K. Mo, and Y. Halpern, *J. Am. Chem. Soc.*, **94**, 551 (1972).
- (14) (a) S. G. Lias, J. R. Eyley, and P. Ausloos, *Int. J. Mass Spectrom. Ion Phys.*, **19**, 219 (1976); (b) J. R. Eyley, P. Ausloos, and S. G. Lias, *J. Am. Chem. Soc.*, **96**, 3673 (1974).
- (15) G. S. Hammond, *J. Am. Chem. Soc.*, **77**, 334 (1955).
- (16) The fact that sulfur might be a better  $\pi$  donor than oxygen in certain excited states of some organic compounds was pointed out by Mangini; see A. Mangini and R. Passerini, *Gazz. Chim. Ital.*, **84**, 606 (1954); A. Mangini, *Rev. Chim.*, **1**, 313 (1962); A. Mangini, *Mem. Accad. Lincei*, in press.
- (17) H. C. Brown and R. R. Holmes, *J. Am. Chem. Soc.*, **78**, 2173 (1956).
- (18) J. M. Miller and M. Onyszchuk, *Can. J. Chem.*, **42**, 518 (1964); E. Gore and S. S. Danyluk, *J. Phys. Chem.*, **69**, 89 (1965).
- (19) R. G. Pearson, "Hard and Soft Acids and Bases", Dowden, Hutchinson, and Ross, Stroudsburg, Pa., 1973; R. G. Pearson, *J. Chem. Educ.*, **45**, 581 (1968).
- (20) G. Klopman and R. F. Hudson, *Theor. Chim. Acta*, **8**, 165 (1967).

# Stereoelectronic Properties of Photosynthetic and Related Systems. 1. Ab Initio Quantum Mechanical Ground State Characterization of Free Base Porphine, Chlorin, and Ethyl Pheophorbide *a*

Dale Spangler,<sup>1,2</sup> Gerald M. Maggiora,\*<sup>3</sup> Lester L. Shipman,<sup>4</sup> and Ralph E. Christoffersen\*<sup>1</sup>

Contribution from the Departments of Chemistry and Biochemistry, University of Kansas, Lawrence, Kansas 66045, and the Chemistry Division, Argonne National Laboratory, Argonne, Illinois 60439. Received December 30, 1976

**Abstract:** Ab initio SCF calculations on the ground state of free base porphine, chlorin, and ethyl pheophorbide *a* have been carried out using the molecular fragment procedure. Molecular orbital energies and ordering, and the correlations of specific orbitals among the molecules studied, have been examined in detail. Ionization potentials have been estimated, and the first ionization potentials are 6.8, 6.4, and 6.4 eV for porphine, chlorin, and ethyl pheophorbide *a*, respectively. The calculations show the expected approximate separation of the HOMO, HOMO - 1, LUMO, and LUMO + 1 from the remainder of the MO manifold in keeping with the "four orbital" model, and isodensity contour plots of occupied and unoccupied molecular orbitals indicate a striking similarity in the "shapes" of these orbitals in all three molecules. Charges and bond orders have been examined. In porphine and chlorin, the bonding picture includes an extended  $\pi$  system whose path of conjugation involves the atoms of the interior of the macrocycle, including the nitrogens and methine carbons. Also, relatively localized  $\pi$  bonds are found between the exterior carbon atoms of the pyrrole moieties. In ethyl pheophorbide *a*, the  $\pi$  bonds of the keto carbonyl of ring V and the vinyl group of ring I are mostly localized, but the path of conjugation within the macrocycle is somewhat less clear. Finally, molecular electrostatic isopotential maps have been constructed and an analysis of the long-range electrostatic field and its relationship to intermolecular interactions is discussed.

Photosynthesis involving either plants or bacteria is well known to be one of the most important energy-conversion mechanisms carried out by living systems. In converting solar to chemical energy and in maintaining the oxygen balance in our biosphere, photosynthesis plays a crucial role. Hence, a detailed understanding of the primary processes that govern photosynthetic energy conversion is of great importance, both to an understanding of fundamental biological processes and to the development of alternate energy sources based on biomimetic conversion of solar energy.

Chlorophyll molecules play a central role in the primary events<sup>5</sup> of photosynthesis. The majority of chlorophyll molecules act cooperatively as an antenna to absorb light and funnel the electronic excitation energy to a "reaction center", where charge separation occurs involving a few special chlorophyll molecules.<sup>6</sup> Although much is now known about the role of chlorophyll in photosynthetic energy conversion, there is still little known about the geometric arrangement and collective electronic structure of associated chlorophyll molecules in the photosynthetic membrane.